# DYNAMICAL BEHAVIOUR OF SINE LOGISTIC SYSTEM IN MANN ORBIT

**Monika Bai[1], Ashish[2*], Pooja Bhatia[3], and Monia[4]**

**Abstract**
By virtue of enormous properties of discontinuous chaos and their reactivity to the earliest conditions, the discontinuous unidimensional equations are applied boundless in numerous applications of engineering and science like weather forecasting, cryptography, security system etc. This paper concerns with the study of the Sine logistic map through Mann orbit, which is a superior feedback technique. In this examination, we found that the growth rate parameter $r$ is inversely proportional to the parameter $\alpha$, that is, as we decrease the parameter $\alpha$, the value of $r$ increases rapidly. Here, we executed Mann iterative procedure on the Sine logistic map by performing time-series evaluation, period- doubling graphs, functional plots and by calculating Lyapunov exponents. We investigated the dynamic properties of the superior system for different values of parameter $\alpha = 0.9$, 0.6, and 0.4.

**Keywords:** Difference equations, chaos, Lyapunov exponents, bifurcation plots.

[1*,3] Department of Mathematics, Baba Mastnath University, Asthal Bohar, Rohtak-124001, India
[1]Email: monikachauhan199530@gmail.com,
[3]Email: poojabudhiraja@bmu.ac.in
[2]Department of Mathematics, Government College, Satnali, Mahendergarh-123024, India
[2]Email: akrmsc@gmail.com , [*]Corresponding author
[4]Department of Mathematics, Government College Kosli, Haryana, India
[4]Email: mndhaka92@gmail.com

***Corresponding Author:** Ashish
Department of Mathematics, Government College, Satnali, Mahendergarh-123024, India
Email: akrmsc@gmail.com

**DOI:**10.53555/ecb/2022.11.4.072

## 1. Introduction

Nowadays, in the discipline of automation and science, the implementation of disorder and its hypothesis have attained considerable thinking of scientists and researchers. Interesting fact on chaos theory and about the nonlinear dynamics is given by Poincare [27] that, in nonlinear systems, if there is a minute change in the initial conditions then it can give drastic change in the output conditions. Hence, in the nonlinear dynamics the examination of far-reaching circumstances is impossible. Mann [22] in 1953 described an iterative procedure to find fixed point of functions, this method demonstrated as superior method in mathematics. P. F. Verhuslt [30] had given a sample of population growth which is popular as logistic map $rx(1-x)$, which executes crucial role in the examination of dynamic behaviour of nonlinear maps. In 1978, M. Feigenbaum [18] investigated the mathematical model of chaos theory which popularize the logistic map. For further learning about chaos and logistic map one may can go along with [ S. H. Strogotz [29], A. C. Luo [21], G. Datseris and U. Parlitz [17] and T. N. Blair [11]].

It was crucial development in the chaos theory in twentieth century. The chaos theory in nonlinear dynamical system contributes various applications in engineering and science like as cryptography, weather forecasting, security system and traffic control model and many more. Many mathematicians discovered different types of one-dimensional logistic maps. The breakthrough in the dynamics of chaotic maps was finding the convergence rate of dynamic maps using Mann procedure. Later, the same equation was studied using Ishikawa procedure by B. Parsad and K. Katiyar [26]. They evaluate time-series graphs, period-doubling plots and computing Lyapunov exponents for describing the properties of the logistic map. The multiplicative map that is originated from the standard logistic map is studied using bifurcation plots and Lyapunov exponents by D. Aniszewska [1] in 2018. A. G. Radwan et al. [19] designed a double humped logistic equation that is used in generating deterministic-random number key. J. Cao [3] investigated the dynamic characteristics of logistic map by adding an extra parameter with the control parameter that improves the dynamic properties of the map. Then in 2022, he also studied a generalised cubic map [16]. Ashish et. al. [7] investigated an approach to regulate disorder behaviour in unidimensional maps. The dynamics of q-deformed logistic map was observed by J. S. Canovas and M. Guillermo [13]. Next year, they again determine the dynamics of q-deformed Gaussian map [14]. In 2020, the stability analysis of generalised logistic map using Mann orbit is described by Khamosh et. al. [20]. A system was defined by using two logistics maps and then examined the existence and stability of fixed points by J. S. Canovas [12] in 2022. In that year, Monika et al. [25] determined the dynamical characteristics of Sine logistic map via Picard orbit. Ashish et al. [10] used Euler's Algorithm to examine the maximum Lyapunov exponent of the nonlinear dynamical systems.

Recently, during 2020-23 Ashish et. al. presented a series of quality investigation. R. Chugh et. al. [6] discussed the dynamic properties of a modulated logistic equation via superior method in 2021. Dynamical properties of a logistic type difference equation and discrete difference map by using superior method, a simple unidimensional map that depends on three control parameters and standard logistic map using Euler's algorithm is demonstrated by Ashish et. al. [2, 4, 8, 23, 24]. In 2023, J. Cao and Ashish [15] observed the behaviour of fixed and periodic states for a map which is a combination of two maps: the conventional map and the Euler's map. In 2023, Ashish et. al. [5] studied stability analysis of unidimensional map by using Noor orbit. For controlling chaos in discrete dynamical systems, a hybrid chaos control method is used by Ashish and M. Sajid [9] in 2023.The dynamical characteristics of q-deformed logistic map using superior approach is examined by Renu et al. [28]. The way of dynamical systems is used to examine the bifurcations of phase portraits and observe the allexact solutions for two systems by Rogers et al. [31].

This proposal introduce step forward by using Mann orbit for the analysis of dynamic properties of Sine logistic map. This analysis is classified into four parts. First section deals with introduction of the paper and brief literature review. Section 2 is the important part of the article; we performed analysis experimentally and computationally and observations are noticed. Section three is about the study of Lyapunov exponent calculation with a few examples. In the last section, we put all the results and conclusion of the analysis.

## 2. Experimental Analysis

In this portion, we observed the theoretical properties about Sine logistic map under superior iteration. Mann orbit is known as a powerful tool for solving non-linear maps. Let us define, $f_r(x) = rx(1-\sin x)$, where $x \in [0,2]$ and $r$ denotes the positive fixed growth rate parameter, this is known as the Sine logistic map. For the initial value $x_0 \in [0,2]$, assuming $x_1$ be the new output, then according to Mann orbit it gives,

$$x_1 = (1-\alpha)x_0 + \alpha f_r(x_0), \text{ where } f_r(x_0) = rx_0(1-\sin x_0)$$

or we can rewrite,

$$x_n = (1-\alpha)x_{n-1} + \alpha r x_{n-1}(1-\sin x_{n-1}) = M_{\alpha,r}(x_n), \quad (1)$$

for all $x_n \in [0,2]$, α ∈ (0,1) and *n* ∈ *N*.

Above system is also called as superior system which is dependent on two control parameters *r* and *α*. For *α* = 1, the above system converts into simple system same as in Picard's orbit and for *α* = 0, there is no change in the system. During the analysis of this superior system, we use *α*∈(0, 1) all through this study. For genuineness of this paper, we suppose *α* = 0.9, 0.6 and 0.4 to investigate the dynamic behaviour of the Sine logistic map.

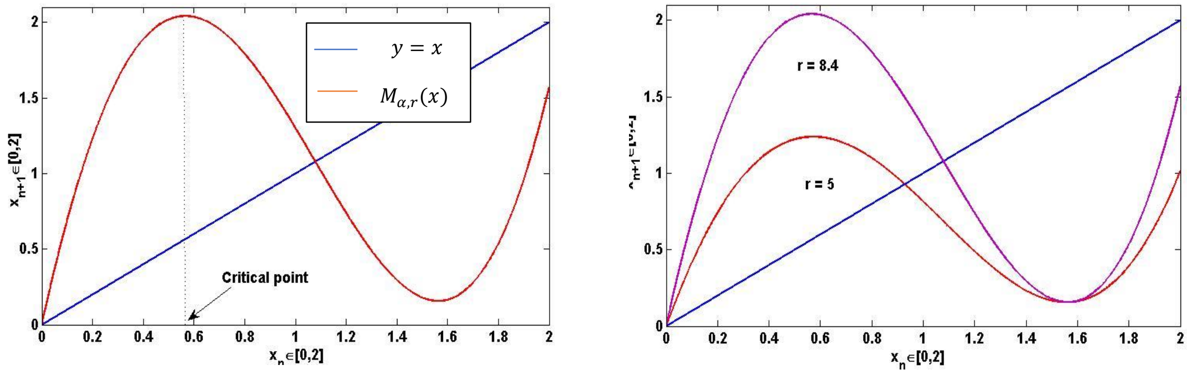


(a) (b

**Figure.1** (a) Functional plot for the system for *r* = 8.4, (b) Functional plot for the system for *r* = 8.4 and 5.

In Figure 1(a) displays functional plot of Sine logistic map and line y = x. The cutting point of these will give fixed point of the superior system. Superior system is given as,

$$M_{\alpha,r}(x) = (1-\alpha)x + \alpha r x(1-\sin x), \quad \text{where } \alpha \in (0, 1) \text{ and } x \in [0, 2].$$

Now, we must calculate fixed point using,

$$f(x) = x,$$

Then, $(1-\alpha)x + \alpha r x(1-\sin x) = x,$

$$x[(1-\alpha) + \alpha r(1-\sin x) - 1] = 0,$$

Either $x = 0$ or $(1-\alpha) + \alpha\, r\,(1-\sin x) - 1 = 0,$

$$-\alpha + \alpha\, r\,(1-\sin x) = 0,$$

$$r(1-\sin x) = 1,$$

$$\sin x = 1 - \frac{1}{r},$$

$$x = \sin^{-1}(1-\frac{1}{r}).$$

Thus, $x = 0$ and $x = \sin^{-1}(1-\frac{1}{r})$ are two fixed points of the Sine logistic map.

### 2.1. Time-series expansion for system $M_{\alpha,r}(x)$ for *α* = 0.9, 0.6, and 0.4

From the examination of unidimensional maps, the nature of the non-linear dynamical system always affected by the control parameter *r*. Hence, in this section we studied in detail about the dynamics of empirical system analysed in the range of the parameter *α* and *r*. Moreover, we have observed the chaotic behaviour of the system for *α* = 0.9, *α* = 0.6 and *α* = 0.4, the system goes into disorder when the parameter *r* lies *r* > 5.3492, *r* > 9.9392 and *r* > 15.1 respectively.

For *α* = 0.9, for 0 ≤ *r* ≤ 3.9584, the whole system approaches to a unique stable stationary point $\sin^{-1}(1-\frac{1}{r})$, it is clearly shown in Figure 2(a). For r > 3.9584, Figure 2(b) displays the system vibrates between two stable solutions up to r ≤ 5.0088. Further, as the parameter approaches, r ≅ 5.3492, the entire system converts into non-periodicity upto r ≤ 8.4 which is displayed in Figure 2(c). Similarly, for α = 0.6, the stability, periodicity and irregularity lie in 0 ≤ r ≤ 11.2. The entire system approaches to a single fixed point $\sin^{-1}(1-\frac{1}{r})$ for 0 ≤ r ≤ 6.0846, and exhibits period-2 and period-3 solution for the prescribed range 6.0846 < r ≤ 9.4015 and 10.6956 < r ≤ 10.847 respectively, graphic Figure 2(d) exhibits the fixed state for the superior system for α = 0.6. The whole system transforms into chaos for r ≅ 9.9392. The chaotic region for α = 0.6 is displayed in Figure 2(e).

Eventually, we observe the chaotic pattern for one more parameter value, α = 0.4. The entire dynamical properties happen for the growth rate parameter 0 ≤ r ≤ 18.1. At this point, the system remains in its stable state for 0 ≤ r ≤ 10.2315 and obtains periodic state for 10.2315 < r ≤ 15.0938. Finally reaches to chaos as parameter approaches to 15.1. The chaotic region for α = 0.4 is displayed in Figure 2(f).

**Remark 2.1.** By examining the time-series plots for the system $M_{\alpha,r}(x)$, it is understood that as the parameter α is inversely proportional to the parameter r, i.e., the growth rate parameter increases consequently up to 69.5 as the parameter α decreases from 1 to 0. For higher value of parameter r, it is amazing to know that the irregular behaviour occurs regularly in all cases.

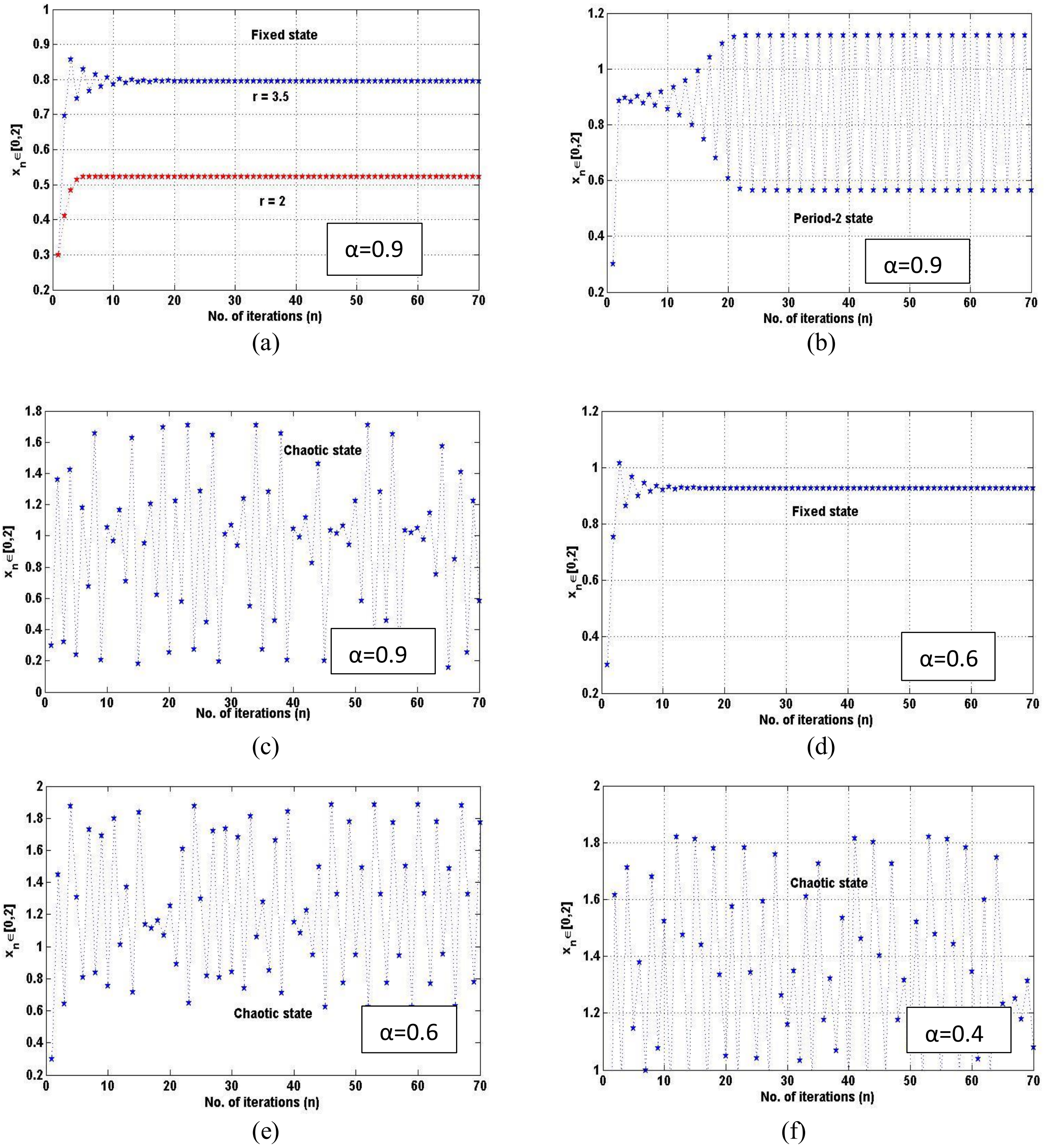


**Figure.2** (a) Stable solution plot for the system $M_{\alpha,r}(x)$ for r = 2 and 3.5, (b) Period-2 state for the system $M_{\alpha,r}(x)$ for r = 4.5, (c) Chaotic region for the system $M_{\alpha,r}(x)$ for r = 7, (d) Fixed point solution for the system $M_{\alpha,r}(x)$ for r = 5, (e) Chaotic region for the system $M_{\alpha,r}(x)$ for r = 10.5, (f) Chaotic region for the system $M_{\alpha,r}(x)$ for r = 16.

## 2.2 Bifurcation Analysis for α = 0.9, 0.6, 0.4, and 0.1

By using equation (1), we examine the bifurcation plots of sine logistic map under Mann iteration for various values of α. The nature of the map totally depends on the parameter r and α. Here, we fix the initial value $x_0 = 0.3$.

**(a) For α = 0.9**

The parametric range for α = 0.9, lies in 0 < r ≤ 8.4. The very first bifurcation occurs at r = 3.9584 and for 0 < r ≤ 3.9584, the system shows the stable behaviour. As r > 3.9584, the system starts vibrating between two stable points $P_1$ and $P_2$, which is also known as initial bifurcation of order two, it extends up to r ≤ 5.0088. As we further increase the parameter r, i.e., for r > 5.0088, again the period-doubling bifurcation of order-4 exists for 5.0088 < r ≤ 5.2862. $P_1$ and $P_2$ splits into $P_{11}$, $P_{12}$ and $P_{21}$,$P_{22}$ respectively upto r < 5.2862. Now, the third period-doubling bifurcation of order-8 occurs when 5.2862 < r ≤ 5.3492 and this pattern remains same of order $2^n$.

It is interesting to notice that as the parameter r approaches up to 5.3492, the whole system grants transformation from period-doubling to chaos. For the parametric range, 5.3492 < r ≤ 8.4, the entire vision of chaos has been seen.

**(c) For α = 0.4**

Similarly, the bifurcation nature of the system for α = 0.4 is also demonstrated. It is observed that the system exhibits its regular and irregular behaviour for 0 < r ≤ 18.1. The systems show stable behaviour for 0 < r ≤ 10.2315. For r > 10.2315, the system splits into periodicity of order 2 up to r ≤ 14.1975. As further r increases, the periodicity of order-4 is seen for 14.1975 < r ≤ 14.940 and periodic window of order-8 is seen for 14.94 < r ≤ 15.0938.

**(b) For α = 0.6**

The regular and irregular nature of the system varies as the growth rate parameter changes from 0 < r ≤ 11.2. The initial bifurcation is observed for r = 6.0846 and for parameter lies in 0 < r ≤ 9.4015, the periodicity is examined in the system of order $2^n$. Here, the vision of period-3 window is also seen for 10.6956 < r ≤ 10.847, which is the most important property of the system which implies chaos. Further, as the parameter r approaches up to 9.9392, the entire beauty of chaos has been seen.

Similarly, periodicity of order $2^n$ has been seen. The elegance of period-3 region is observed for 17.0765 < r ≤ 17.65. For r ≅ 15.1, irregularity is observed that is the place of infinite bifurcation.

**(d) For α = 0.1**

For α = 0.1, the parameter approaches up to 69.5, i.e., for 0 < r ≤ 69.5, the system displays stable behaviour. But as we increase r > 69.5, the nature of the system cannot be described.

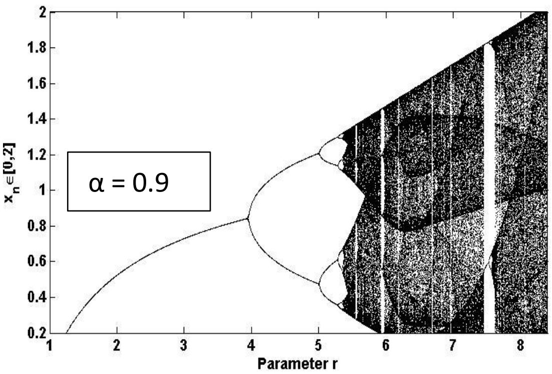


(a)

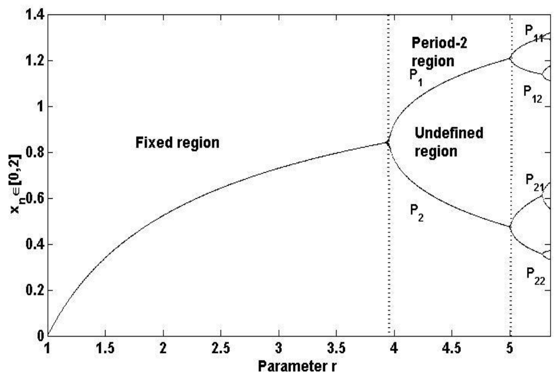


(b)

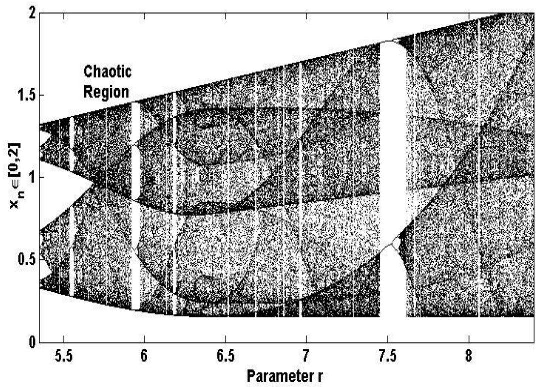


(c)

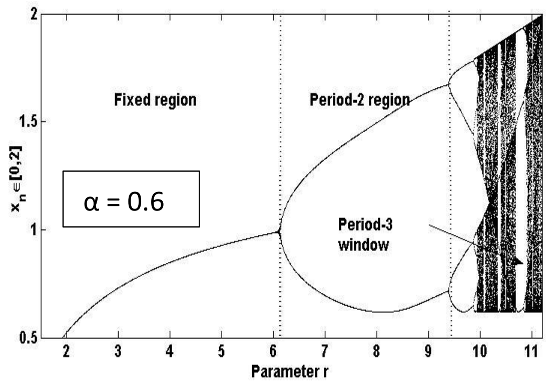


(d)

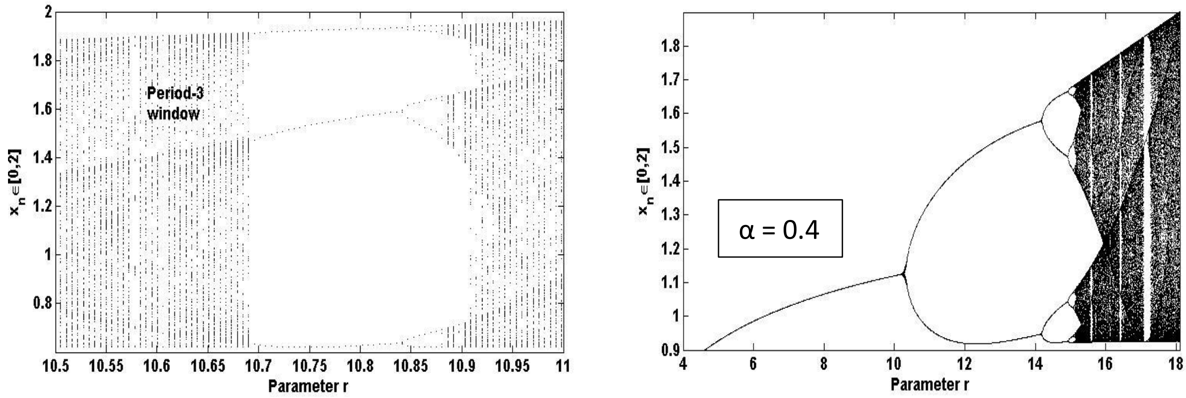


(e) (f)

**Figure 3.** (a) Bifurcation plot for the system for r ∈ [0, 8.4] and α = 0.9, (b) Periodic representation for the system for r ∈ [1, 5.3492], (c) Chaotic region for the system for 5.3492 < r ≤ 8.4, (d) Periodic plot for the system for r ∈ [0, 11.2] and α = 0.6, (e) Period-3 window for the system for r ∈ (10.6956, 10.847] and α = 0.6, (f) Bifurcation plot for the system for r ∈ [0, 18.1].

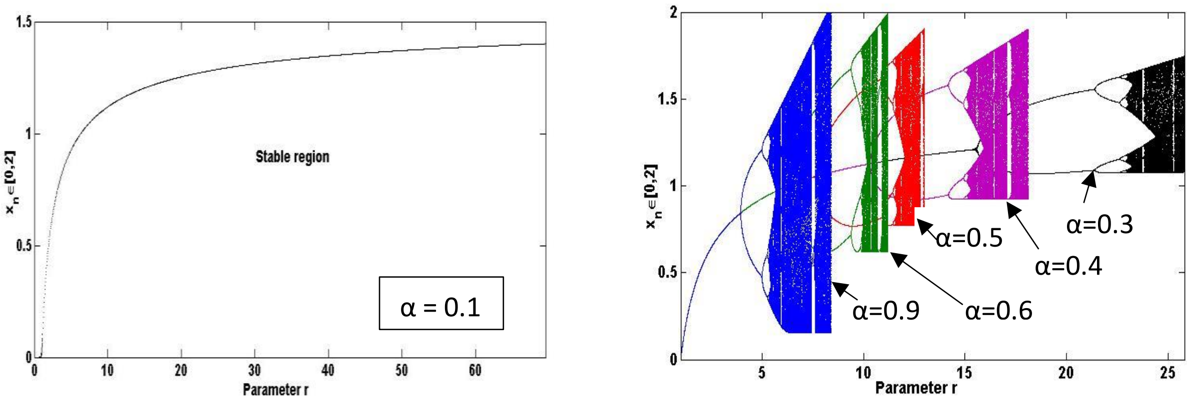


(a) (b)

**Figure 4.** (a) Stable region for the system for r ∈ [0, 69.5] and α = 0.1, (b) Comparative representation of bifurcation plot

**Remark 2.2.** From bifurcation analysis, it is observed that there exists period-3 window in all cases except for α = 0.9. For α = 0.9, bifurcation and chaos start at r 3.95 and r = 5.34 respectively while this value extends as r = 6.08 and r = 9.9 for α = 0.6 and r = 10.23 and r = 15.1 for α = 0.4.

**Remark 2.3** For α = 0.1, there is only stable region for 0 < r ≤ 69.5. For r > 69.5, there is undefined region.

**3. Lyapunov Exponent**

In the previous section, we observed the chaotic properties of the Sine logistic equation in superior orbit by evaluating bifurcation and time-series graphs for three different values of parameter α = 0.9, 0.6 and 0.4. Now, we have one more technique to determine the properties of difference maps that is the Lyapunov Exponent. Lyapunov Exponent is applied to calculate the susceptible relativity of two trajectories which are initialising from very close basic points. It calculates the rate of convergence approaching the fixed point for stable periodic nature and it computes the rate of divergence among the trajectories for chaotic behaviour. Under the Mann iteration, for the Sine logistic map the Lyapunov exponent is described in the subsequent manner:

Let us suppose two starting point $x$ and $x+\varepsilon$, where $\varepsilon \in (0,1)$. Now the exponential expansion $\varepsilon e^{n\sigma}$ is calculated as divergence $\gamma$ between two orbits and n represents the numerous iterations. Now, this can be written as,

$$M^n_{\alpha,r}(x+\varepsilon) - M^n_{\alpha,r}(x) = \gamma = \varepsilon e^{n\sigma},$$
$$\frac{M^n_{\alpha,r}(x+\varepsilon)}{\varepsilon} - \frac{M^n_{\alpha,r}(x)}{\varepsilon} = e^{n\sigma}. \quad (4.1)$$

Now, putting limit $\varepsilon \to 0$, we get

$$\lim_{\varepsilon\to 0}\left(\frac{M^n_{\alpha,r}(x+\varepsilon)}{\varepsilon} - \frac{M^n_{\alpha,r}(x)}{\varepsilon}\right) = e^{n\sigma},$$
$$(M^n_{\alpha,r})'(x) = e^{n\sigma}. \quad (4.2)$$

Now, by taking logarithm on both side we get,

$$\sigma = \frac{1}{n}\log\left|(M_{\alpha,r}^{n})'(x)\right| \quad (4.3)$$

where r > 0, α ∈ (0,1) and initial derivation of $M_{\alpha,r}^{n}(x)$ is given by $(M_{\alpha,r}^{n})'(x)$.

The nth- degree polynomial can be differentiated by using chain rule,

$$(M_{\alpha,r}^{n})'(x_1) = (M_{\alpha,r}^{n})'(x_n)\,.\,(M_{\alpha,r}^{n})'(x_{n-1}) \ldots\ldots (M_{\alpha,r}^{n})'(x_2).\,(M_{\alpha,r}^{n})'(x_1). \quad (4.4)$$

Then from (4.3) and (4.4), we get

$$\sigma = \frac{1}{n}\log\left|\begin{matrix}(M_{\alpha,r}^{n})'(x_n)\,.\,(M_{\alpha,r}^{n})'(x_{n-1})\\ \ldots\ldots (M_{\alpha,r}^{n})'(x_2).\,(M_{\alpha,r}^{n})'(x_1)\end{matrix}\right|,$$

$$= \frac{1}{n}[\log\left|(M_{\alpha,r}^{n})'(x_n)\right| + \log\left|(M_{\alpha,r}^{n})'(x_{n-1})\right| + \cdots + \log\left|(M_{\alpha,r}^{n})'(x_2)\right| + \log\left|(M_{\alpha,r}^{n})'(x_1)\right|$$

$$= \frac{1}{n}\sum_{i=1}^{n}\log\left|M_{\alpha,r}{}'(x_i)\right|, \quad (4.5)$$

In general, for stable point of $M_{\alpha,r}(x)$, equation (4.5) transforms to

$\sigma = \log\left|M_{\alpha,r}(x)\right|$.

Lyapunov exponent for the periodic orbit of order-p is,

$$\sigma = \frac{1}{p}\sum_{i=1}^{p}\log\left|M'_{\alpha,r}(x_i)\right|. \quad (4.6)$$

**Remark 3.1** The fixed and periodic trajectories are stable if $\sigma < 0$ and if $\sigma > 0$, then periodic and fixed trajectories are said to be unstable. Hence, stability and instability or orbits is measured by the Lyapunov exponent.

**Example 3.1** Evaluate the Lyapunov exponent for the superior system $M_{\alpha,r}(x)$, for the equation $f_r(x) = rx(1-\sin x)$, where $r \in [0, 7.5]$ and $x \in [0, 2]$. When we take,
(i) r = 3.5 and α = 0.9 and
(ii) r = 4.5 and α = 0.9.

**Solution (i).** From earlier section, it is understood that for system $M_{\alpha,r}(x)$, for α = 0.9 and r = 3.5, the trajectory of the map is fixed and this fixed-point value is given by $\sin^{-1}(1-\frac{1}{r}) = 0.7956$. Now, for the fixed orbit, to measure the Lyapunov exponent, we have to solve equation (4.6).

$$M_{\alpha,r}(x) = (1-\alpha)x + \alpha.r.x.(1-\sin x)$$

$$M'_{\alpha,r}(x) = (1-\alpha) + \alpha.r.(1-\sin x) - \alpha\, r\, x\, \cos x$$

$$= 1 - \alpha + \alpha.r.(1 - \sin x - x\cos x)$$

$$M'_{0.9,3.5}(0.7956) = 1 - 0.9 + 0.9 \times 3.5 \times [1 - \sin(0.7956) - 0.7956 \times \cos(0.7956)]$$

$$= -0.7533$$

Now, by using eq (4.6), we get, $\sigma = \log|-0.7533| = -0.1230$

Hence, for r = 3.5, the observed Lyapunov exponent value is – 0.1230, that is a negative quantity, thus according to the description of Lyapunov exponent the orbit is stable attracter.

**(ii)** When 3.958 < r ≤ 5.0088, periodic nature of period-2 is exhibited by the orbit of the map $M_{\alpha,r}(x)$. Thus, for r = 4.5, $x_1 = 0.5657$ and $x_2 = 1.1196$ are two examined periodic points. Now, we find

$$M'_{\alpha,r}(x_1) = 1 - 0.9 + 0.9 \times 4.5 \times [1 - \sin(0.5657) - 0.5657 \times \cos(0.5657)] = 0.4453$$

$$M'_{\alpha,r}(x_2) = 1 - 0.9 + 0.9 \times 4.5 \times [1 - \sin(1.1196) - 1.1196 \times \cos(1.1196) = -1.4718$$

Now, by using equation (4.6), we get

$$\sigma = \frac{1}{2}[\log\left|M'_{\alpha,r}(x_1)\right| + \log\left|M'_{\alpha,r}(x_2)\right|]$$

$$= \frac{1}{2}[\,\log|0.4453| + \log|-1.4718|\,]$$

$$= \frac{1}{2}\,[\,0.1678 + (-0.3513)$$

$$= -0.0917.$$

Hence, in this case also Lyapunov exponent is negative and thus periodic points are stable attracter. Figure 5(a) displays the behaviour of Lyapunov exponent for the system for α = 0.9, the higher value of Lyapunov exponent reaches up to 0.8 in Mann procedure while it reaches to 0.9 for the same in Picard orbit as shown in Figure 5(c). For 5.36 < r ≤ 8.4, the system displays a negative Lyapunov exponent value which indicates the unstable chaotic region as displayed in Figure 5(b). The original system admits Lyapunov exponent higher than Lyapunov exponent in superior system, this implies that the system acquires weaker sensitivity for lower Lyapunov exponent value.

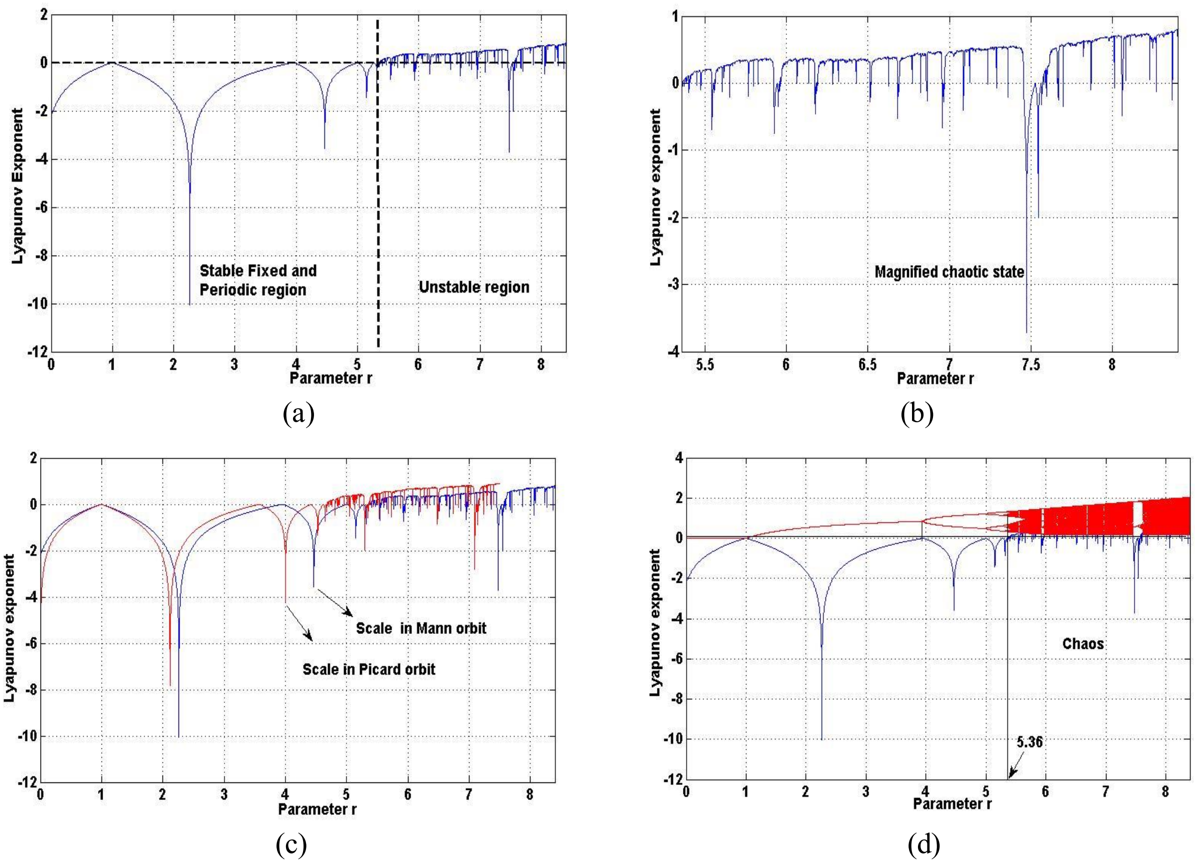


**Figure 5**. (a) Lyapunov exponent plot for the system $M_{\alpha,r}(x)$ for α = 0.9 and 0 ≤ r ≤ 8.4, (b) Magnified chaotic region for the system $M_{\alpha,r}(x)$, (c) Comparison plot of Lyapunov exponents of the Sine logistic map in Picard orbit and Mann orbit, (d) Comparison plot of bifurcation and Lyapunov exponent for the system $M_{\alpha,r}(x)$.

## 4. Conclusion

In this portion, all conclusion about Sine logistic map in Mann orbit is discussed briefly. The entire dynamics depends on the two controls parameter *r* and *α*. The following results are concluded: The transformation from regularity to irregularity is described by using bifurcation plots and time-series diagrams. The dynamical behaviour is demonstrated for the control parameter *α* = 0.9, 0.6, and 0.4. We observed that the period-3 window exists for 10.6956 < r ≤ 10.847 and 17.0765 < r ≤ 17.65, when we take for α = 0.6 and α = 0.4, respectively. While it does not exist in the case for α = 0.9. Lyapunov exponent is calculated for some value of parameters *r* and *α*, and a graphical representation is also demonstrated in the Section 3.

## References


1. D. Aniszewska, New discrete chaotic multiplicative maps based on the logistic map, Int. J. of Bifurcat. Chaos, 2018, 28(09), 185118.
2. Ashish and A. Malik, Dynamical Interpretation of Logistic Map using Euler's Numerical Algorithm, Chaos Theory and Applications, 2022, 4(3), 128-134.
3. Ashish and J. Cao, A novel fixed point feedback approach studying the dynamical behaviours of standard logistic map, Int. J. of Bifurcat. Chaos, 2019, 29(01), 1950010.
4. Ashish, J. Cao, and F. Alsaadi, Chaotic evolution of difference equation in Mann orbit, J. Appl. Anal. and Comput., 2021, 11(6), 3063-3082.
5. Ashish, J. Cao, and M. A. Noor, Stabilization of fixed points in chaotic maps using Noor orbit with applications in cardiac arrhythmia, J. Appl. Anal. and Comput, 2023, 13(5), 2452-2470.
6. Ashish, J. Cao, and R. Chugh, Discrete chaotification of a modulated logistic system, Int. J. of Bifurcat. Chaos, 2021, 31(05), 2150065.
7. Ashish, J. Cao, and R. Chugh, Controlling chaos superior feedback system and its applications in discrete traffic model, Int. J. Fuzzy Syst., 2019, (21), 1467-1479.
8. Ashish, Renu, and R. Chugh, On the dynamics of a discrete difference map in Mann orbit, Comp. Appl. Math, 2022, (41) (226), 1-19.

9. Ashish and M. Sajid, Stabilization in Chaotic maps using hybrid chaos control procedure, Heliyon Journal, 2023, (10) (2), e23984.
10. Ashish, Monia, Manoj Kumar, Khamosh and A. K. Malik, Lyapunov exponent using Euler's Algorithm with Applications in Optimal Transportation Problems, Yugoslav Journal of Operations Research, August 2022, (32) (4), 503-513.
11. T. N. Blair, Nonlinear Dynamics and its Applications, Magnum Publishing, 2018.
12. J. S. Canovas, The Dynamics of Coupled Logistic maps, Netw. Heterogen. Med., 2022, 18, 275-290.
13. J. S. Canovas and M. Guillermo, On the Dynamics of q-deformed Logistic map, Physics Letters A, 2019, 383, 1742-1754.
14. J. S. Canovas and M. Guillermo, On the Dynamics of q-deformed Gaussian map, International Journal of Bifurcation and Chaos, 2020, 30(8), 2030021.
15. J. Cao and Ashish, Scaling analysis at transitions of chaos driven by Euler's numerical algorithm, International Journal of Bifurcation and Chaos, 2023, 33(8), 2350092, 13 pages.
16. J. Cao and Ashish, Dynamical Interpretations of a generalised cubic map, Journal of Appl. Anal. Comput., 2022, 12, 2314-2329. G. Datseris and U. Parlitz, Nonlinear Dynamics, Springer Nature, Switzerland, 2022.
17. M. J. Feigenbaum, Quantitative universality for a class of nonlinear transformations, Journal of statistical physics, 1978, 19(1), 25-52.
18. S. M. Ismail, L. A. Said, A.G. Radwan, A.H. Madian, and M. F. Abu-Elyazeed, Generalized double-humped logistic map-
28. S. H. Strogotz, Nonlinear Dynamics and Chaos, CRC Press, New York, 2018.
29. P. F. Verhulst, La loi d'accroissement de la population, Nouveaux Memories de l'Académie Royale des Sciences et Belles-Lettres de Bruxelles, 1845, 14-54.
30. Y. Zhou and J. Li, Bifurcations and exact solutions in the model of nonlinear electrodynamics of materials with strong ellipticity condition, Springer, 2023, 112, 1-13.
based medical image encryption, Journal of advanced research, 2018, 10, 85-98.
19. V. Kumar, Khamosh and Ashish, An empirical approach to study the stability of generalized logistic map in superior orbit, Adv. Math.: Sci. J. 2020, 9(10), 8356-8374.
20. A. C. Luo, Resonance and Bifurcation to Chaos in Pendulum, Southern Illinois University Edwardsville, USA, 2018.
21. W. R. Mann, Mean value methods in iteration, Proc. Amer. Math. Soc., 1953, 4, 506-510.
22. K. Mokni and M. Chaoni, Complex Dynamics and bifurcation analysis for a Benerton-Holt population model with Alee effect, Int. J. Biomath, 2023, 16, 2250127.
23. Monia, Ashish, M. Kumar, and A. K. Malik, Effect of Modulating Parameters in Chaos and Lyapunov Exponent, Mathematical Statistician and Engineering Applications, 2022, 71(32), 1213-1223.
24. Monika, Ashish and Pooja Bhatia, Dynamical Interpretations of Sine Logistic Map using Picard Orbit, Neuro-Quantology, 2022, (20) (13), 4142-4151.
25. B. Parsad and K. Katiyar, A stability analysis of logistic model, International Journal of Nonlinear Sciences, 2013, 71-79.
26. H. Poincaré, Les méthodes nouvelles de la mécanique celeste, Gauthier-Villars et fils, Imprimeurs-libraires, 1899, (3).
27. Renu, Ashish and R. Chugh, Dynamics analysis and implication of q-deformed logistic map via superior approach, Journal of Applied Nonlinear Dynamics, 2023, 12(2), 285-296.